1-6-2012

Accelerated magnetosheath flows caused by IMF draping: Dependence on latitude

Nikolai V. Erkaev
Russian Academy of Sciences

Charlie J. Farrugia
University of New Hampshire, Charlie.Farrugia@unh.edu

Alexander V. Mezentsev
Siberian Federal University

Roy B. Torbert
University of New Hampshire, roy.torbert@unh.edu

Helfried K. Biernat
Austrian Academy of Sciences

Comments

This is an article published by AGU in Geophysical Research Letters in 2012, available online: https://dx.doi.org/10.1029/2011GL050209

Accelerated magnetosheath flows caused by IMF draping: Dependence on latitude

N. V. Erkaev,[1,2] C. J. Farrugia,[3] A. V. Mezentsev,[2] R. B. Torbert,[3] and H. K. Biernat[4,5]

Received 1 November 2011; revised 25 November 2011; accepted 28 November 2011; published 6 January 2012.

[1] In previous work we used a semi-analytical treatment to describe accelerated magnetosheath flows caused by the draping of interplanetary magnetic field (IMF) lines around the magnetosphere. Here, we use the same approach, i.e., modeling the magnetic field lines as elastic strings, to examine how the magnetic tension force, one of the two agents responsible for producing these flows, varies along field lines away from the equatorial plane. The bend in the field line caused by the draping mechanism propagates as two oppositely-directed waves to higher latitudes. For a due northward IMF - the case we consider here - these propagate symmetrically north/south of the equatorial plane. As a result, a two-peaked latitude velocity profile develops as we go further downtail and the velocity peaks migrate along the magnetic field line to higher latitudes. We examine this velocity-profile for two Alfvén Mach numbers (M_A = 8 and 3), representative of conditions in the solar wind at 1 AU ("normal" solar wind and solar transients). Qualitatively, the picture is the same but quantitatively there are important differences: (i) the flows reach higher values for the lower M_A (maximum V/V_{SW} = 1.6) than for the higher M_A (V/V_{SW} = 1.3); (ii) asymptotic values are reached farther downstream of the dawn-dusk terminator for the lower M_A ($\sim -50\ R_E$ vs $-15\ R_E$); (iii) For the lower M_A the highest speeds are reached away from the equatorial plane. We predict two channels of fast magnetosheath flow next to the magnetopause at off-equatorial latitudes that exceed the solar wind speed. **Citation:** Erkaev, N. V., C. J. Farrugia, A. V. Mezentsev, R. B. Torbert, and H. K. Biernat (2012), Accelerated magnetosheath flows caused by IMF draping: Dependence on latitude, *Geophys. Res. Lett.*, *39*, L01103, doi:10.1029/2011GL050209.

1. Introduction

[2] The observation of accelerated magnetosheath flows not related to magnetic reconnection was reported a long time ago [*Howe and Binsack*, 1972]. Over the years other researchers have examined such flows [*Chen et al.*, 1993; *Petrinec and Russell*, 1997]. That the stagnation line flow, which is characteristic of the near-magnetopause magnetosheath for northward interplanetary magnetic field (IMF) [*Sonnerup*, 1974], leads to enhanced plasma speeds perpendicular to the upstream field was pointed out by *Phan et al.* [1994] and *Farrugia et al.* [1998]. Recently there has been an upsurge of interest in these accelerated flows, which could reach values exceeding the solar wind speed (V_{SW}) by a considerable amount. This interest arose from data examples showing strongly accelerated flows ($V/V_{SW} \sim 1.5$) [*Rosenqvist et al.*, 2007; *Lavraud et al.*, 2007] which, though few, were compelling enough to call for explanation. The physical explanation of these accelerated flows has been addressed from two angles: global MHD simulations [*Lavraud et al.*, 2007], and semi-analytical work [*Erkaev et al.*, 2011, hereinafter Paper 1].

[3] The aim of this paper is to show that there are further important ramifications which have not previously been considered. In our semi-analytic treatment, the magnetic field lines obey equations similar to that of a stretched string, leading to their designation as magnetic string equations [*Erkaev*, 1988; Paper 1, and references therein]. From the string formulation there emerges the possibility of propagating waves. This is particularly relevant here since, as they drape around the magnetosphere, bends develop in the field lines. These can then propagate along the field lines as MHD waves. The question then is what effect, if any, do they have on the accelerated flow profile?

2. Results

2.1. The Magnetic String Equation

[4] The shape of the magnetic field lines around the magnetosphere is described by the magnetic string equations, which are second order, hyperbolic partial differential equations. They read as follows (see further details in Paper 1; and by *Farrugia et al.* [1995])

$$\frac{\partial^2 \mathbf{r}}{\partial \tau^2} = \frac{1}{M_A^2}\frac{\partial}{\partial \alpha}\left(\rho \frac{\partial \mathbf{r}}{\partial \alpha}\right) - \frac{1}{\rho}\nabla \Pi. \qquad (1)$$

Here $\mathbf{r}$ is the position vector, ρ is the mass density, M_A, the Alfvén Mach number, and Π is the total pressure, i.e., the sum of the magnetic and plasma pressures. All quantities are normalized to their solar wind values. The coordinate system (α, τ, ξ) is defined such that coordinate α varies along the magnetic field lines, τ varies along the flow streamlines, and ξ varies along the electric field lines ($\mathbf{E} = -\mathbf{v} \times \mathbf{B}$). So these coordinates are related to the physical quantities ($\mathbf{V}$, $\mathbf{B}$, $\mathbf{E}$). The right hand side of (1) contains two force terms and, as explained in Paper 1, which concentrated on to the equatorial plane, it is the cooperation followed by the competition between these two forces which first accelerates the plasma and then causes it to reach a terminal speed equal to the solar wind speed.

[1]Institute of Computational Modeling, Russian Academy of Sciences, Krasnoyarsk, Russia.
[2]Siberian Federal University, Krasnoyarsk, Russia.
[3]Space Science Center and Department of Physics, University of New Hampshire, Durham, New Hampshire, USA.
[4]Space Research Institute, Austrian Academy of Sciences, Graz, Austria.
[5]Institute of Physics, Karl-Franzens-University of Graz, Graz, Austria.

0094-8276/12/2011GL050209

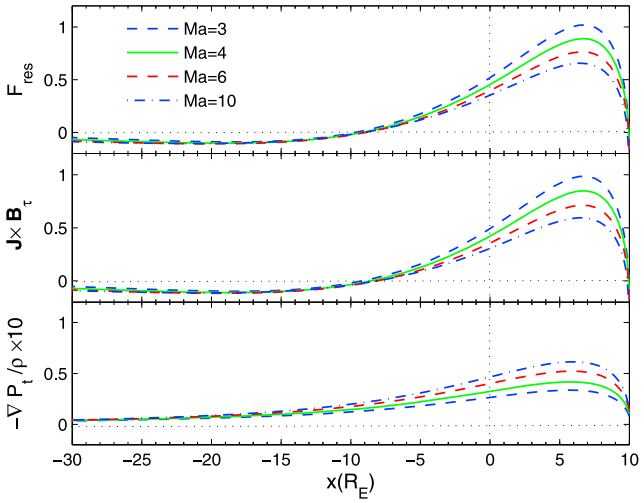

Figure 1. The equatorial profiles as a function of X (in Earth radii, R_E) of (top) the resultant force; (middle) the Lorentz force tangential to the magnetopause; and (bottom) the plasma pressure gradient force. The X-axis is directed from Earth to Sun, positive sunwards. The curves are parametrized by the Alfvén Mach number, as indicated in Figure 1 (top).

[5] To visualize this, we show in Figure 1 (top) the sum of the two forces (F_{res}) as a function of distance X (in R_E) from the Earth in the equatorial plane (Z = 0). As in Paper 1, the calculation is based on an IMF pointing due north. The shape of the magnetosphere is that of *Shue et al.* [1998]. The four curves are parametrized by the Alfvén Mach number M_A. All curves have a maximum in F_{res}, whose size depends on M_A and which is reached on the dayside, followed by a gradual decrease on the nightside. The two forces cancel each other at $X \sim -9\ R_E$ and the maximum speed is reached there. After that the resultant force is negative, i.e., points sunward, and the flows are decelerated until they reach the solar wind speed far downtail.

[6] For completeness, we show in Figure 1 (middle) the Lorentz force $\mathbf{J} \times \mathbf{B}$ tangential to the surface. The difference between the Lorentz force and the resultant force is just the gradient of the plasma pressure (Figure 1, bottom; multiplied by 10), which is small in the magnetic barrier. With increasing M_A, the contribution of the pressure gradient increases while that of the Lorentz force decreases.

2.2. Development of a Two-Humped Latitude Flow Profile

[7] We work with two M_A's (3, 8) and start with $M_A = 3$. This would generally correspond to passage at Earth of magnetically-dominated configurations, the most common of which are interplanetary coronal mass ejections (ICMEs) [*Neugebauer and Goldstein*, 1997, and references therein] and their subset, magnetic clouds [*Burlaga et al.*, 1981].

[8] Figure 2 shows the draped configuration of magnetic field lines (blue) and the flow streamlines (green) for $M_A = 3$. The vertical axis labeled Z is along the external magnetic field direction and points north, and the horizontal axis is the X axis directed from Earth to Sun, positive sunward. The field lines at Z = 0 are initially convex sunward (to the right) and thus produce a tailward-pointing force due to field line tension. Tailward of $X \leq -9\ R_E$ they become convex tailward and then produce a sunward force, decelerating the plasma.

[9] Away from the Z = 0 plane the situation is, however, different. Far from Z = 0 (the *XY* plane), the field line has developed two points of inflection because the bend at Z = 0 has propagated symmetrically north and south and thereby deformed the field line. At X-distances where the field is convex tailward at low latitudes it is still convex sunward at higher Z values. Therefore forces develop at higher latitudes which are now pointing tailward and thus adding to the total pressure gradient force. This is different from what is happening at Z = 0 where the forces are still opposed and decelerate the plasma. Thus the peak accelerated flows migrate north/south of the *XY* plane. This migration is with respect to the magnetic field line. Since magnetic field lines are being dragged tailward by the flow, between two adjacent field lines the high speeds have moved northward and southward. The red blobs refer to the location of maximum speeds.

[10] Figure 3 shows the flow profiles along the magnetic field lines at 8 different X-values in the range [= 3 R_E (brown), −24 R_E (red)]. The vertical axis points along the external field (north), and the horizontal axis is the ratio V/V_{SW}. Tailward of $X = -9\ R_E$, the maximum speeds start to move away from the equatorial plane to higher northern and southern latitudes, while still remaining, of course, close to the magnetopause. The peak speeds continue to increase with increasingly negative X in the range shown.

[11] As we see, the profile changes from being single-peaked in latitude (for lines 1–4) to being double-peaked, symmetric about the equatorial plane. Further, the peaks separate from each other such that the further downstream

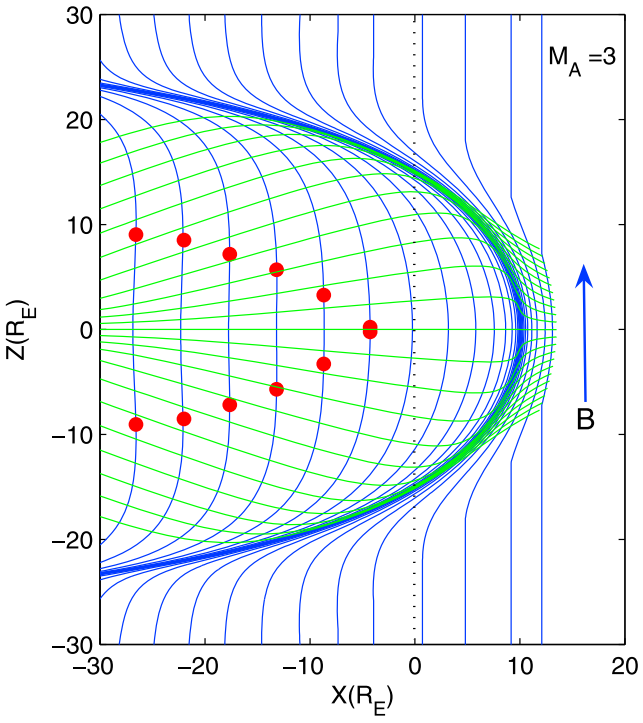

Figure 2. An *XZ* projection of the draped configuration of magnetic and flow stream lines. Magnetic field lines are in blue and flow streamlines in green. The plane Z = 0 is the equatorial plane. The magnetic field upstream of the bow shock points north (arrow). Red blobs indicate the location of maximum speeds. The result is for $M_A = 3$.

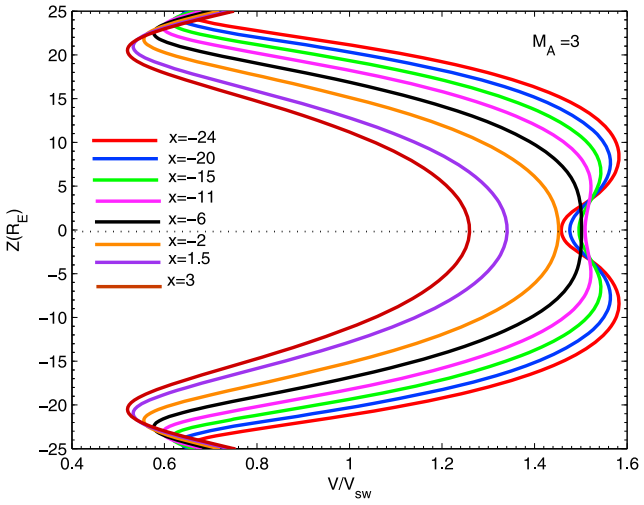

Figure 3. The velocity profiles along the magnetic field lines for M_A = 3. The vertical axis, Z, points north, along the external field. The velocities are normalized to the solar wind speed. Eight values of X in the range [3, −24] R_E are shown by different colors.

one goes the further north/south that they lie. Importantly, the ratio of the maximum magnetosheath speed (V) to that of the solar wind V_{SW} increases with downtail distance. Thus V/Vsw = 1.52 (X = −11 R_E) and 1.58 (X = −24 R_E). The lines approach V = V_{SW} as the field lines approach the bow shock at both ends of the figure.

[12] This acceleration mechanism is to be contrasted with that of the equatorial situation shown in Figure 1. As explained above, at Z = 0 the acceleration resulted from cooperation followed by competition of the two forces in the magnetic string equation. By contrast, north or south of the points of inflection in the field line, both the total pressure gradient force as well as the magnetic tension force point in the same (tailward) direction. For that reason the asymptotic behavior is different (see further below).

[13] Figure 4 shows the corresponding figure for M_A = 8, in a format similar to that of Figure 3. Again, we note a pronounced two - humped Z speed profile developing after

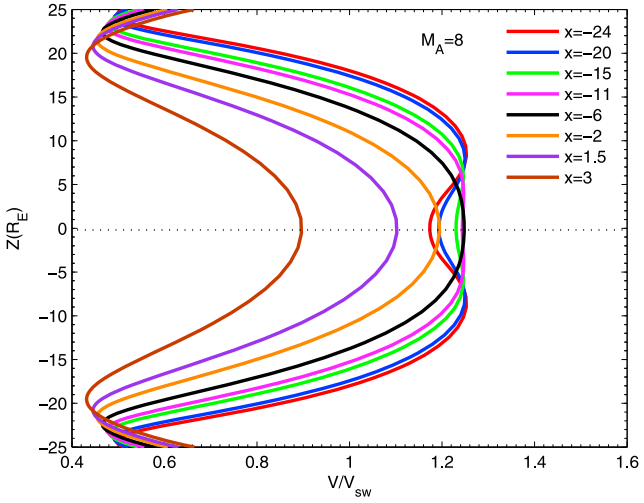

Figure 4. Similar to Figure 3 but for M_A = 8.

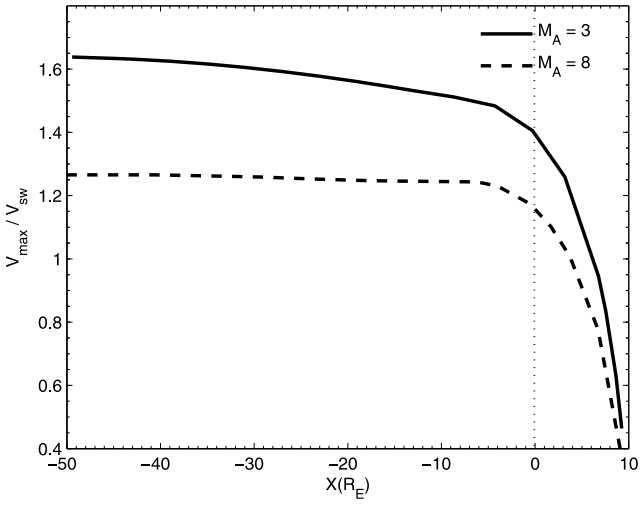

Figure 5. The maximum magnetosheath flow speed ratio for two Alfvén Mach numbers: M_A = 3 (solid line) and M_A = 8 (dashed) as a function of X. It illustrates that the asymptotic behavior of this quantity as one goes further downtail depends strongly on M_A. In both cases, the maximum asymptotic flow speed is higher than the solar wind speed.

$X \approx -9R_E$. The maximum values of V_{SW} at all downtail distances is smaller than for M_A = 3, reaching up to only 1.25 V_{SW}. This is a combined effect of weaker magnetic tension and weaker pressure gradient force. We also note that, contrary to the case for M_A = 3, these maximum accelerated flows at higher north/south latitudes barely exceed values at Z = 0.

[14] What happens to these accelerated flows as we go even further downstream than X = −30 R_E? Figure 5 shows the result for the two Alfvén Mach numbers (dashed: M_A = 8, solid trace: M_A = 3). In both cases the flow speeds approach an asymptotic value, which is higher for M_A = 3 (= 1.58 V_{SW} for M_A = 3 versus 1.25 V_{SW} for M_A = 8). Asymptotic values are reached nearer Earth for M_A = 8 than for M_A = 3. The asymptotic behavior comes about because at large negative X the bends in the field lines straighten out, reducing the magnetic tension force, while simultaneously the pressure gradient force decreases.

3. Summary and Discussion

[15] We have discussed new aspects of accelerated flows due to IMF draping around the magnetosphere. These arise away from the equatorial plane and are related to the propagation of the field bend to higher north/south latitudes. The resulting two-humped velocity profile typically sets in at X ∼ −10 R_E. The accelerated flows here are strongly dependent on the solar wind Alfvén Mach number upstream of Earth's bow shock. The mechanism has some important differences with that which occurs at the equatorial plane. In particular we find that it reaches a terminal velocity higher than that of the solar wind.

[16] The chosen M_A - (3, 8) - are representative of a wide range of conditions at the near-Earth solar wind: M_A = 8 is fairly typical of the "normal" solar wind, and M_A = 3 is, in turn, fairly representative of ICMEs and their subset, magnetic clouds.

[17] The work illustrates how fruitful the magnetic string formalism has proved to be. We have predicted a flow behavior, which is subject to experimental verification, based on what we model as a string.

[18] A question arises as to the possibility of mistaking these draping-related accelerated flows at high latitudes for an IMF pointing north with those that might result from reconnection poleward of the cusp. The latter are typically associated with an ionospheric convection pattern where the flows over the poles are sunward, so called "reverse convection" [*Maezawa*, 1976; *Crooker*, 1992]. So in experimental work on these flows close to the magnetopause it is important to exclude those which are due to high-latitude reconnection by checking that there is no reverse convection pattern.

[19] We studied the case when the IMF is pointing due north. This was done for ease of visualization. If the IMF has a non-zero Y-component, the result would be the same: the vertical axis still points along the IMF direction in the (YZ) plane, and what we call the equatorial plane is tilted by the clock angle of the IMF (i.e., the polar angle in the YZ plane).

[20] An implication is that at very large downtail X values we should have two channels of high speed magnetosheath flow in this case, which are particularly pronounced for low Alfvén Mach number. At other latitudes, the magnetosheath flows are at solar wind speeds. This is still subject to experimental verification.

[21] **Acknowledgments.** This work was done while NVE was on a research visit to the Space Science Center of UNH. This work is supported by RFBR grant N 09-05-91000-ANF _a, and also by the Austrian "Fonds zur Förderung der wissenschaftlichen Forschung" under Project I 193-N16 and the "Verwaltungsstelle für Auslandsbeziehungen" of the Austrian Academy of Sciences. Work by CJF was supported by NASA grants NNX10AQ29G and NNX08AD11G.

[22] The Editor wishes to thank Steven Petrinec and an anonymous reviewer for their assistance evaluating this paper.

References

Burlaga, L., E. Sittler, F. Mariani, and R. Schwenn (1981), Magnetic loop behind an interplanetary shock: Voyager, Helios, and IMP 8 observations, *J. Geophys. Res.*, *86*(A8), 6673–6684.

Chen, S.-H., M. G. Kivelson, J. T. Gosling, R. J. Walker, and A. J. Lazarus (1993), Anomalous aspects of magnetosheath flow and of the shape and oscillations of the magnetopause during an interval of strongly northward interplanetary magnetic field, *J. Geophys. Res.*, *98*(A4), 5727–5742.

Crooker, N. U. (1992), Reverse convection, *J. Geophys. Res.*, *97*(A12), 19,363–19,372.

Erkaev, N. V. (1988), Results of the investigation of MHD flow around the magnetosphere, *Geomagn. Aeron.*, *28*, 455–464.

Erkaev, N. V., C. J. Farrugia, B. Harris, and H. K. Biernat (2011), On accelerated magnetosheath flows under northward IMF, *Geophys. Res. Lett.*, *38*, L01104, doi:10.1029/2010GL045998.

Farrugia, C. J., N. V. Erkaev, H. K. Biernat, and L. F. Burlaga (1995), Anomalous magnetosheath properties during Earth passage of an interplanetary magnetic cloud, *J. Geophys. Res.*, *100*(A10), 19,245–19,257.

Farrugia, C. J., H. K. Biernat, N. V. Erkaev, L. M. Kistler, G. Le, and C. T. Russell (1998), MHD model of magnetosheath flow: Comparison with AMPTE/IRM observations on 24 October, 1985, *Ann. Geophys.*, *16*, 518–527.

Howe, H. C., Jr., and J. H. Binsack (1972), Explorer 33 and 35 plasma observations of magnetosheath flow, *J. Geophys. Res.*, *77*(19), 3334–3344.

Lavraud, B., J. E. Borovsky, A. J. Ridley, E. W. Pogue, M. F. Thomsen, H. Rème, A. N. Fazakerley, and E. A. Lucek (2007), Strong bulk plasma acceleration in Earth's magnetosheath: A magnetic slingshot effect?, *Geophys. Res. Lett.*, *34*, L14102, doi:10.1029/2007GL030024.

Maezawa, K. (1976), Magnetospheric convection induced by the positive and negative *Z* components of the interplanetary magnetic field: Quantitative analysis using polar cap magnetic records, *J. Geophys. Res.*, *81*(13), 2289–2303.

Neugebauer, M. and R. Goldstein (1997), Particle and field signatures of coronal mass ejections in the solar wind, in *Coronal Mass Ejections*, *Geophys. Monogr. Ser.*, vol. 99, pp. 245–251, edited by N. Crooker, J.-A. Joselyn, and J. Feynmann, AGU, Washington, D. C.

Petrinec, S. M., and C. T. Russell (1997), Hydrodynamics and MHD equations across the bow shock and along the surfaces of planetary obstacles, *Space Sci. Rev.*, *79*, 757–791.

Phan, T.-D., G. Paschmann, W. Baumjohann, N. Sckopke, and H. Lühr (1994), The Magnetosheath region adjacent to the dayside magnetopause: AMPTE/IRM observations, *J. Geophys. Res.*, *99*(A1), 121–141.

Rosenqvist, L., A. Kullen, and S. Buchert (2007), An unusual giant spiral arc in the polar cap region during the northward phase of a coronal mass ejection, *Ann. Geophys.*, *25*, 507–517.

Shue, J.-H., et al. (1998), Magnetopause location under extreme solar wind conditions, *J. Geophys. Res.*, *103*(A8), 17,691–17,700.

Sonnerup, B. U. Ö. (1974), The reconnecting magnetopause, in *Magnetospheric Physics*, edited by B. M. McCormac, pp. 23–33, D. Reidel, Norwell, Mass.

H. K. Biernat, Space Research Institute, Austrian Academy of Sciences, Schmiedlstr. 6, A-8042 Graz, Austria.

N. V. Erkaev, Institute of Computational Modeling, Russian Academy of Sciences, Academgorodok 50/44, Krasnoyarsk 660036, Russia. (erkaev@icm.krasn.ru)

C. J. Farrugia and R. B. Torbert, Space Science Center, University of New Hampshire, Morse Hall, Durham, NH 03857, USA.

A. V. Mezentsev, Institute of Computational Modeling, Siberian Federal University, Krasnoyarsk 660041, Russia.